



Article

Charge-Discharge Properties of the Surface-Modified ZrNi Alloy Electrode with Different Degrees of Boiling Alkaline Treatment

Akihiro Matsuyama ^{1,2,*}, **Hironori Mizutani** ¹, **Takumi Kozuka** ¹ and **Hiroshi Inoue** ²¹ Advanced and High Functional Products Development Division, Aichi Steel Corporation, Tokai, Aichi 476-8666, Japan; h-mizutani@he.aichi-steel.co.jp (H.M.); takumi@he.aichi-steel.co.jp (T.K.)² Department of Applied Chemistry, Graduate School of Engineering, Osaka Prefecture University, Sakai, Osaka 599-8531, Japan; inoue-h@chem.osakafu-u.ac.jp

* Correspondence: a-matsuyama@he.aichi-steel.co.jp; Tel.: +81-52-603-9741

Academic Editor: Hua Kun Liu

Received: 2 August 2016; Accepted: 22 September 2016; Published: 28 September 2016

Abstract: Charge-discharge properties of the surface-modified ZrNi negative electrodes with different degrees of boiling alkaline treatment were investigated. The boiling alkaline treatment was performed by immersing the ZrNi electrode in a boiling 6 M KOH aqueous solution for 2 h or 4 h. The initial discharge capacity for the untreated ZrNi negative electrode was $21 \text{ mAh}\cdot\text{g}^{-1}$, but it was increased to $114 \text{ mAh}\cdot\text{g}^{-1}$ and $308 \text{ mAh}\cdot\text{g}^{-1}$ after the boiling alkaline treatments for 2 h and 4 h, respectively. The discharge capacity for the ZrNi negative electrode after the treatment for 2 h steadily increased with repeating charge-discharge cycles as well as that of the untreated electrode, whereas that for the ZrNi negative electrode after the 4 h treatment greatly decreased. The high rate of dischargeability was improved with an increase in the treatment period of time, and the charge-transfer resistance was drastically decreased. Scanning electron microscopy (SEM) and electron dispersive X-ray spectroscopy demonstrated the ZrO_2 passive layer on the ZrNi alloy surface was removed by the boiling alkaline treatment to form a porous morphology containing Ni(OH)_2 , which can be reduced to Ni during charging, leading to the reduction of a barrier for the charge-discharge reactions.

Keywords: ZrNi; hydrogen storage alloy; negative electrode; nickel-metal hydride (Ni-MH) battery; boiling alkaline treatment

1. Introduction

The nickel-metal hydride (Ni-MH) battery is one of the most important devices for energy storage. AB_5 -type rare earth alloys have been commercially used as negative electrode active materials, and have exhibited good battery performances with strong rate capability and cycle stability [1,2]. However, for increasing the energy density of Ni-MH batteries, the hydrogen storage capacity needs to be improved, which gives us a motivation to develop new high-capacity hydrogen storage alloys. So far, high-capacity hydrogen storage alloys such as ZrMn_2 (AB_2)-type Laves phase alloys [3,4], Mg-based alloys [5,6], $\text{La}_2\text{Mg}_1\text{Ni}_9$ (AB_3)-type super lattice alloys [7,8], TiNi-type alloys [9] and V-based body-centered cubic (BCC)-type alloys [10] have been developed.

The ZrNi alloy is expected as a new high-capacity negative electrode active material for the Ni-MH battery because it has a hydrogen storage capacity of about 2.0 mass% H_2 [11,12], which corresponds to a charge capacity of $536 \text{ mAh}\cdot\text{g}^{-1}$. The discharge capacity of the ZrNi alloy negative electrode, however, has been very low so far [13,14], because the passive ZrO_2 layer on the alloy surface inhibited hydrogen absorption into the alloy [15,16]. The surface structures of alloys as well as their composition influence the battery performance, including the initial activity, maximum discharge

capacity, rate capability and charge-discharge cycle stability. Therefore, various techniques such as mechanical milling [17,18], melt spinning to make the surface amorphous [19], alkaline or acidic treatment to remove the passive layer [20–22], fluorination treatment [23] and electroless coating [24] have been utilized for the modification of the surface structure or composition. The alkaline treatment, in which LaNi₅-based alloys and Zr-type Laves phase alloys were immersed in a hot alkaline solution, has been extensively reported as an effective technique for removing the surface passive layer, leading to the improvement of the battery's performance [20,24,25]. Recently, we have reported that the boiling alkaline treatment of the ZrNi alloy negative electrode greatly improved the initial discharge capacity [26].

In this study, we investigated the other negative electrode properties such as the charge-discharge cycle performance, the high rate of dischargeability and the charge-transfer resistance for the ZrNi negative electrodes with the boiling alkaline treatment for different periods of time or different degrees of the treatment effect.

2. Experimental

2.1. Preparation and Surface Treatment of the ZrNi Alloy

The ZrNi alloy ingot was prepared with element constituents (Zr 99.0% and Ni 99.9% purities) by arc-melting in an Ar atmosphere. Before arc-melting, a piece of titanium was melted a few times to remove the residual oxygen in the apparatus. The resultant ingot was annealed at 1173 K for 20 h in an Ar atmosphere, followed by mechanically crushing and sieving between 20 μm and 40 μm in diameter. The resultant alloy powders were immersed in a boiling 6 M KOH alkaline solution for 2 h or 4 h. After the boiling alkaline treatment, the alloy powders were thoroughly rinsed with ion exchange water and then dried in vacuum.

2.2. Electrochemical Measurement of the ZrNi Electrodes with and without the Boiling Alkaline Treatment

The ZrNi negative electrodes with and without the boiling alkaline treatment were prepared as follows. Briefly, the ZrNi powders (42.5 mg) were mixed with Cu powders (5 mg) and 25 μL of 10 wt% polyvinyl alcohol aqueous solution to make a paste. The paste was cast in a porous Ni as a current collector to make a negative electrode. The resultant ZrNi electrode was treated by immersing in a boiling 6 M KOH solution for 2 h or 4 h. The electrolyte solution was a 6 M KOH solution containing 1 M LiOH. The positive and reference electrodes were NiOOH/Ni(OH)₂ and Hg/HgO electrodes, respectively.

In the charge-discharge cycle tests, each negative electrode was charged at 100 $\text{mA}\cdot\text{g}^{-1}$ for 5 h and discharged at 25 $\text{mA}\cdot\text{g}^{-1}$ to the cut off potential of -0.5 V versus Hg/HgO at 303 K or 333 K. After each charging and discharging, the circuit was opened for 10 min. In the rate performance tests, each negative electrode was charged at 100 $\text{mA}\cdot\text{g}^{-1}$ for 5 h and then discharged at 10–200 $\text{mA}\cdot\text{g}^{-1}$ to -0.5 V versus Hg/HgO at 333 K. Electrochemical impedance spectroscopy was performed in a frequency range between 0.1 Hz and 64 kHz with an amplitude of 5 mV after each electrode was charged at 100 $\text{mA}\cdot\text{g}^{-1}$ for 5 h, and then kept at an open-circuit potential for 1 h at 333 K. All electrochemical properties were measured by VMP3 (Bio-Logic, Claix, France).

2.3. Characterization of the ZrNi Alloy with and without the Boiling Alkaline Treatment

The chemical compositions of the ZrNi powders with and without the boiling alkaline treatment were measured by induced couple plasma spectroscopy (ICPs, ICPV-1017, Shimadzu, Kyoto, Japan). Changes surface morphology of the ZrNi powders with and without the boiling alkaline treatment were examined by scanning electron microscopy (SEM, S-4300, HITACHI, Tokyo, Japan) and energy dispersive X-ray (EDX, EMAX, Horiba, Kyoto, Japan) spectroscopy. After the boiling alkaline treatment, the Zr and Ni concentrations in the solution were analyzed by ICPs (SPS4000, Seiko, Tokyo, Japan).

3. Results and Discussion

3.1. Electrochemical Properties of the ZrNi Electrodes with and without the Boiling Alkaline Treatment

Figure 1 shows the initial discharge curves at 303 K and 333 K for the ZrNi negative electrodes with and without the boiling alkaline treatments for 2 h and 4 h. As shown in Figure 1a, at 303 K the initial discharge capacity (C_1) for the untreated ZrNi negative electrode was $9 \text{ mAh}\cdot\text{g}^{-1}$, whereas the C_1 values after the boiling alkaline treatments for 2 h and 4 h were $24 \text{ mAh}\cdot\text{g}^{-1}$ and $89 \text{ mAh}\cdot\text{g}^{-1}$, respectively. On the other hand, at 333 K the C_1 value for the untreated ZrNi negative electrodes was $21 \text{ mAh}\cdot\text{g}^{-1}$, and it increased to $114 \text{ mAh}\cdot\text{g}^{-1}$ and $308 \text{ mAh}\cdot\text{g}^{-1}$ after the boiling alkaline treatments for 2 h and 4 h, respectively, as shown in Figure 1b. Thus, the C_1 value was greatly improved by the boiling alkaline treatment for 4 h.

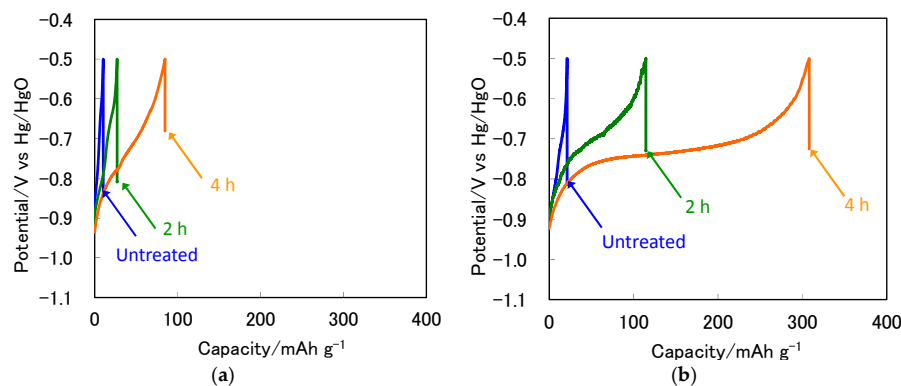


Figure 1. Discharge curves for the ZrNi electrode with and without the boiling alkaline treatment for 2 h and 4 h at (a) 303 K and (b) 333 K.

Figure 2 shows the cycle performance at 333 K for the untreated and treated ZrNi negative electrodes. The discharge capacities of the ZrNi electrodes with and without the boiling alkaline treatment for 2 h steadily increased from $114 \text{ mAh}\cdot\text{g}^{-1}$ to $142 \text{ mAh}\cdot\text{g}^{-1}$ and $21 \text{ mAh}\cdot\text{g}^{-1}$ to $43 \text{ mAh}\cdot\text{g}^{-1}$ for the initial five cycles, respectively, because these electrodes were activated during the charge-discharge cycles. However, after the boiling alkaline treatment for 4 h, the discharge capacity of the ZrNi electrode decreased from $308 \text{ mAh}\cdot\text{g}^{-1}$ to $85 \text{ mAh}\cdot\text{g}^{-1}$ for the initial five cycles. The ZrNi particles were pulverized under $10 \mu\text{m}$ in diameter by the charge-discharge cycling as shown in our previous study [26]. This can lead to the increase in the contact resistance and the decrease in the utilization of alloy particles.

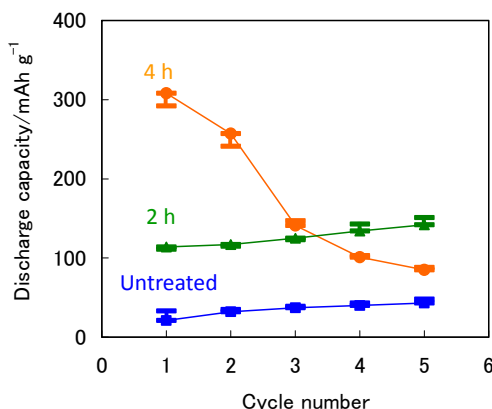


Figure 2. Discharge capacities as a function of the cycle number for the ZrNi negative electrodes with and without the boiling alkaline treatments for 2 h and 4 h at 333 K.

Figure 3 shows the C_1 values as a function of the specific discharge current at 333 K for the untreated and treated ZrNi negative electrodes. The C_1 values at $10 \text{ mA}\cdot\text{g}^{-1}$ and $200 \text{ mA}\cdot\text{g}^{-1}$ for the untreated ZrNi negative electrode were $32 \text{ mAh}\cdot\text{g}^{-1}$ and $14 \text{ mAh}\cdot\text{g}^{-1}$, respectively, whereas those for the ZrNi electrodes after the boiling alkaline treatments for 2 h and 4 h were $175 \text{ mAh}\cdot\text{g}^{-1}$ and $29 \text{ mAh}\cdot\text{g}^{-1}$, and $320 \text{ mAh}\cdot\text{g}^{-1}$ and $98 \text{ mAh}\cdot\text{g}^{-1}$, respectively. These results clearly indicate that the rate performance was greatly improved by the boiling alkaline treatment. However, the discharge capacity greatly decreased more than $25 \text{ mA}\cdot\text{g}^{-1}$ at specific discharge currents. Because the β -hydride ZrNiH and γ -hydride ZrNiH₃ are stable [11,27], they will not easily release hydrogen in the discharge process, leading to slow hydrogen diffusion. Consequently, the electrochemical hydrogen desorption rate will be dominated by the hydrogen diffusion rate, which causes the larger decrease in the discharge capacity at higher specific discharge currents, as shown in Figure 3.

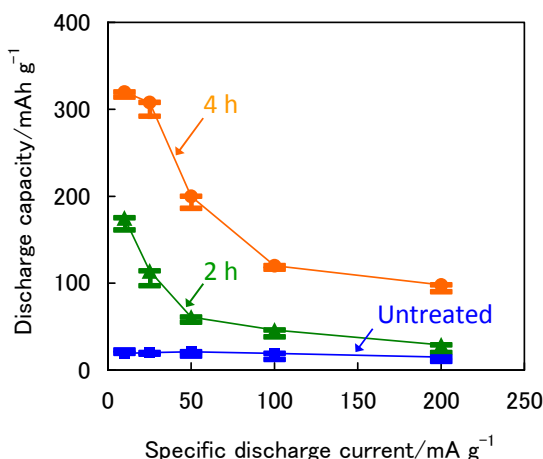


Figure 3. The initial capacities as a function of specific discharge current at 333 K for the ZrNi electrodes with and without the boiling alkaline treatment for 2 h and 4 h.

To confirm the formation of the ZrNi hydrides in the charge process, X-ray diffraction (XRD) profiles after charging and discharging were measured. The XRD profiles after charging and discharging for the ZrNi negative electrodes with and without the boiling alkaline treatment for 4 h are shown in Figure 4. The strong diffraction peaks around 44.8° and 51.8° are due to the Ni current collector. In each electrode the XRD pattern after charging demonstrated the formation of ZrNiH₃ (ICDD Card No. 01-089-2626). After discharging at $25 \text{ mA}\cdot\text{g}^{-1}$, the XRD pattern for the untreated ZrNi negative electrode was similar to that after charging, but the intensity of each peak was a little weak. In addition, some tiny diffraction peaks assigned to ZrNiH (ICDD Card No. 01-084-0567) were also detected. On the other hand, for the treated ZrNi negative electrode, the peak intensity for ZrNiH₃ greatly decreased, and that for ZrNiH was stronger than for the untreated ZrNi negative electrode, suggesting that the dehydrogenation from ZrNiH₃ to ZrNiH in the discharging process was facilitated by the boiling alkaline treatment. However, the peaks for ZrNiH were broad, probably because the crystal structure of the ZrNi alloy was distorted by the absorption and desorption of hydrogen. The complete dehydrogenation from ZrNiH₃ to ZrNiH corresponds to $357 \text{ mAh}\cdot\text{g}^{-1}$, so the conversion from ZrNiH₃ to ZrNiH for the treated ZrNi negative electrode is estimated as 86%.

Figure 5a shows the Nyquist plots after the first charging for the ZrNi negative electrodes with and without the boiling alkaline treatments for 2 h and 4 h. The area surrounded by the broken line in Figure 5a was enlarged, as shown in Figure 5b. The equivalent circuit is shown in Figure 5c. Each Nyquist plot was composed of three depressed semicircles and a straight line [28]. The first semicircle is attributed to the resistance (R_2) and capacitance (C_2) between the alloy particles and the current collector. The second semicircle represents the contact resistance (R_3) and capacitance (C_3) between the alloy particles. The third semicircle represents the charge-transfer resistance (R_4) and

double-layer capacitance (C_4). The straight line is attributable to the hydrogen diffusion in alloy particles, which is called Warburg impedance (W). The intercept at the Z' axis in the high frequency range represents electrolyte resistance (R_1).

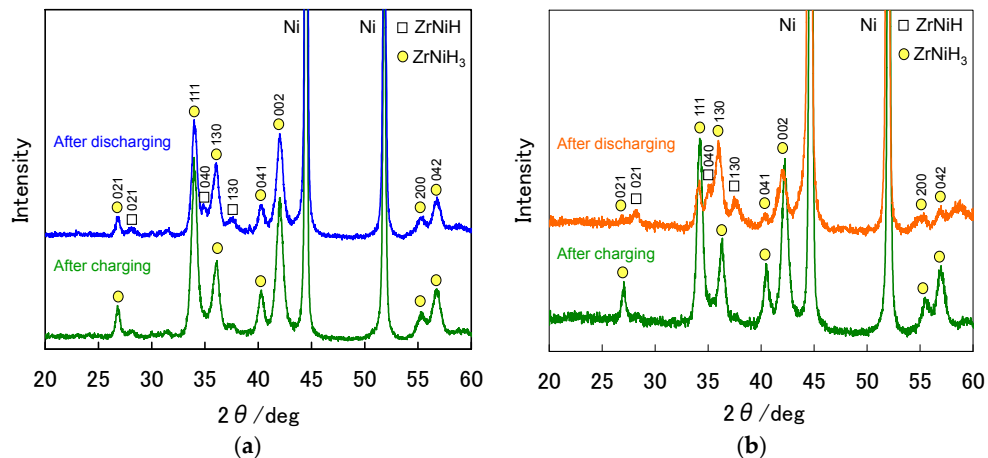


Figure 4. The X-ray diffraction (XRD) profiles after charging and discharging for the ZrNi electrodes: (a) without and (b) with the boiling alkaline treatment for 4 h.

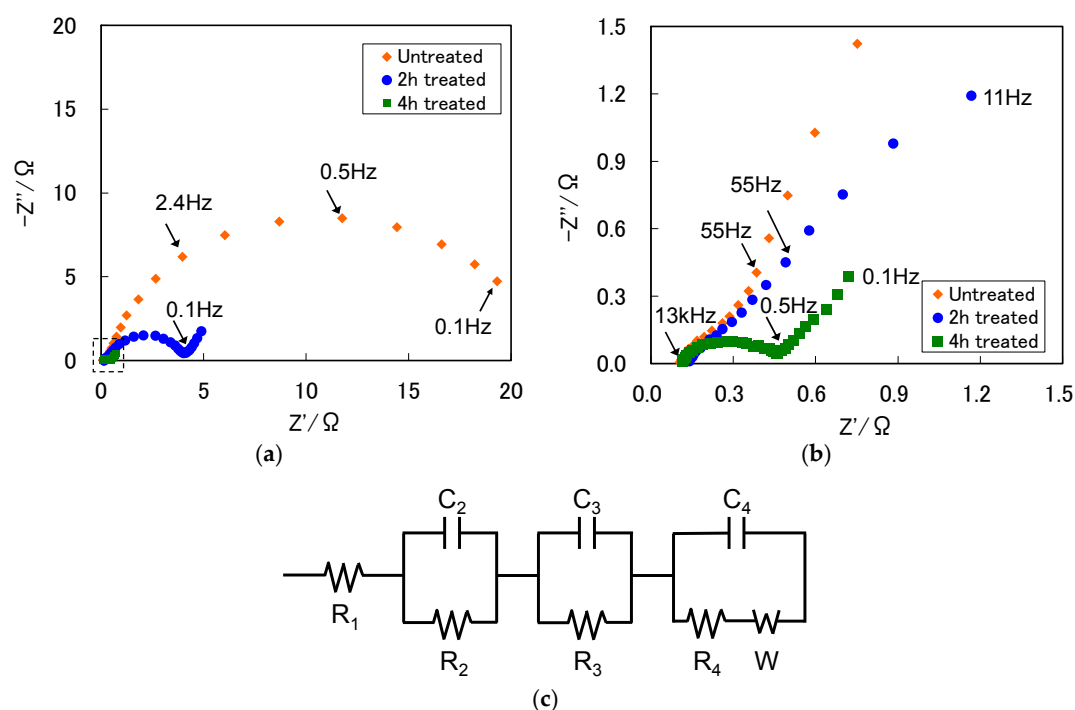


Figure 5. (a) Nyquist plots; (b) enlarged Nyquist plots for the fully charged ZrNi alloys with and without the boiling alkaline treatment for 2 h and 4 h; and (c) equivalent circuit.

Table 1 summarizes resistances (R_1 – R_4) and capacitances (C_2 – C_4), estimated by simulating the equivalent circuit for the ZrNi negative electrodes with and without the boiling alkaline treatments for 2 h and 4 h. In Table 1, R_2 and R_4 significantly decreased with increasing the boiling alkali treatment period of time, whereas C_2 and C_4 increased. On the other hand, R_3 and C_3 were scarcely changed before and after the boiling alkaline treatment, suggesting that the pulverization of alloy particles did not occur during the boiling alkaline treatment but did during charge-discharge cycling [28].

Table 1. Resistances (R_1 – R_4) and capacitances (C_2 – C_4) for the ZrNi negative electrode with and without the alkaline treatment for 2 h and 4 h.

Treatment Time	R_1/Ω	R_2/Ω	R_3/Ω	R_4/Ω	C_2/F	C_3/F	C_4/F
Untreated	0.12	4.39	0.13	16.16	0.017	3.68×10^{-3}	14.76×10^{-3}
2 h	0.12	1.58	0.16	3.62	2.78	3.79×10^{-3}	21.50×10^{-3}
4 h	0.11	0.67	0.11	0.27	3.60	2.04×10^{-3}	75.79×10^{-3}

3.2. Morphology of the ZrNi Alloys with and without the Boiling Alkaline Solution

The chemical compositions of the ZrNi powders with and without the boiling alkaline treatment for 2 h and 4 h by ICPs are shown in Table 2. The composition of the untreated ZrNi powder was equivalent to the theoretical one. The total content was slightly decreased as the treatment time was increased, suggesting that the oxygen content was increased for the untreated ZrNi powder, because ZrO_2 was detected by X-ray photoelectron spectroscopy (XPS) [26]. On the contrary, when the ZrNi powders were treated in the boiling alkaline solution, the contents of Zr and Ni and the Zr/Ni ratio steadily decreased with an increase in the alkaline treatment time, suggesting that both Zr and Ni dissolved during the boiling alkaline treatment, and Zr dissolved faster than Ni. The decrease in total content with an increase in the alkaline treatment time suggests that oxygen was contained in the treated ZrNi powders as $Ni(OH)_2$ and ZrO_2 , because $Ni(OH)_2$ and ZrO_2 were detected after the boiling alkaline treatment by XPS [26].

Table 2. Chemical composition of the ZrNi alloy powers with and without the boiling alkaline treatment for 2 h and 4 h.

Treatment Time	Content/at%		Total	Zr/Ni
	Zr	Ni		
Theoretical	50.00	50.00	100.00	1.00
Untreated	49.76	49.37	99.13	1.00
2 h	48.85	49.78	98.63	0.98
4 h	47.32	48.61	95.93	0.97

Figure 6a–c shows the SEM images of the ZrNi powders with and without the boiling alkaline treatments for 2 h and 4 h, respectively. The elemental analysis for the ZrNi powder surface was performed at 10 points in a row by EDX spectroscopy, and the results are summarized in Figure 6d–f. The surface of the untreated ZrNi powder was uniformly smooth, as shown in Figure 6a. In Figure 6d, the composition at each point of the smooth surface was similar, and the Zr/Ni ratio was almost one regardless of the sampling point.

After the 2 h treatment, the surface of the ZrNi powder consisted of smooth areas (Spots 4, 5, 7 and 10 in Figure 6e), rough areas (Spots 3, 8 and 9 in Figure 6e) and porous areas (Spots 1, 2 and 6 in Figure 6e). As can be seen from Figure 6e, the smooth areas had compositions similar to the untreated powder surface, suggesting that no modification occurred in these areas. During the boiling alkaline treatment some alloy powders were stirred, but others were sunk in the vessel. Therefore, the alloy surface may not have been uniformly modified. In the rough areas, the Zr content decreased and the O content increased. Moreover, in the porous areas, the decrease in Zr content and increase in O content were greater. On the other hand, the Ni content slightly decreased in the rough and porous areas. The Zr/Ni ratio was less than one as a whole. The ICP analysis exhibited that the Zr concentration in the alkaline solution was 7 ppm, and Ni was not detected, suggesting that during the boiling alkaline treatment Zr was oxidized and partially dissolved as $HZrO_3^-$ in the boiling alkaline solution from the rough and porous areas [29]. On the other hand, Ni also seems to be oxidized to $Ni(OH)_2$ [29,30].

After the 4 h treatment, the ZrNi surface mostly changed to a porous morphology, as shown in Figure 6c. The Zr and Ni contents greatly decreased and the O content greatly increased, as shown

in Figure 6f. The ICP analysis showed that the Zr and Ni concentrations in the alkaline solution were 20 ppm and 8 ppm, respectively. These results indicate that the amount of dissolved Zr increased, and part of the oxidized Ni also dissolved as HNI_2^- [29,30], supporting the extensive formation of the porous morphology.

As shown in Figures 1 and 2, the C_1 was greatly increased by the longer boiling alkaline treatment, and the high rate of dischargeability was also improved, as shown in Figure 3. In addition, Table 1 shows that R_4 and C_4 drastically changed. These results are due to the ZrO_2 passive layer on the ZrNi alloy surface being removed to form the porous morphology containing Ni(OH)_2 [26], which can be reduced to metallic Ni during charging [31], leading to the reduction of a barrier for the charge-discharge reactions. The metallic Ni is well known to work as a catalyst for the electrochemical hydrogen desorption reaction [22]. However, C_1 after the boiling alkaline treatment for 2 h was much lower than that after the 4 h treatment. This seems to mean that the residual ZrO_2 inhibited the electrochemical reactions.

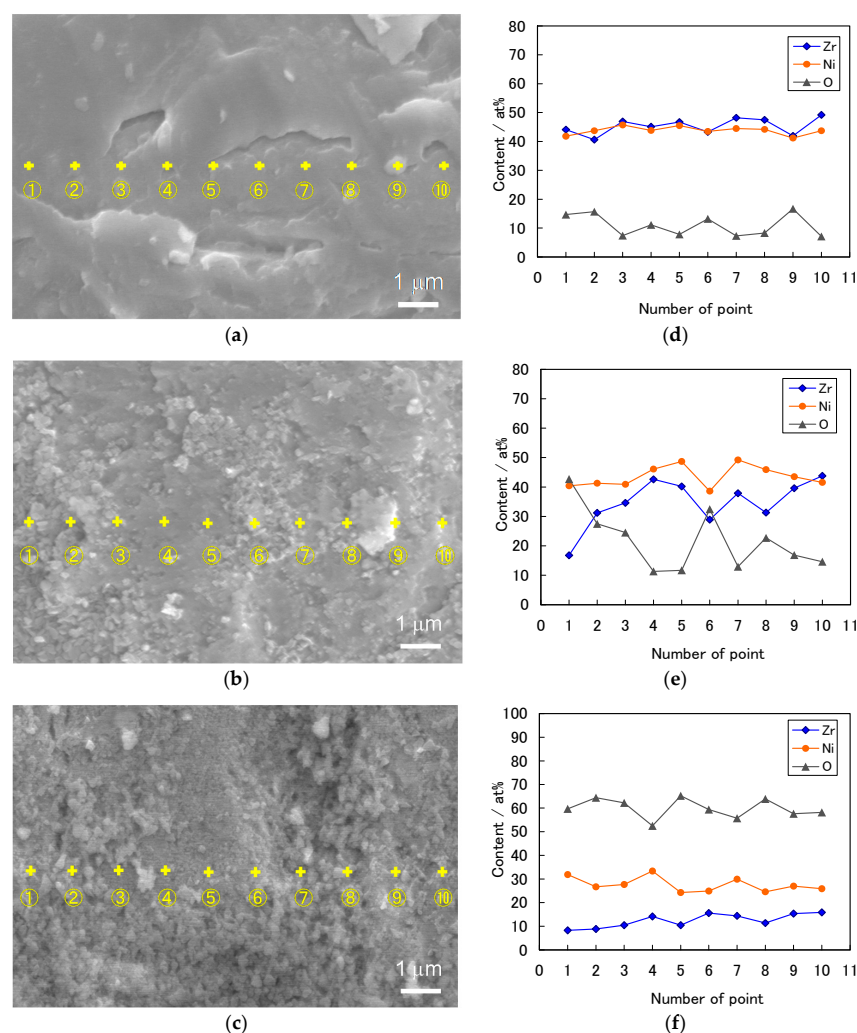


Figure 6. The scanning electron microscopy (SEM) images and Zr, Ni, and O contents at 10 spots analyzed by energy dispersive X-ray (EDX) for the ZrNi alloy powders with and without the boiling alkaline treatments for 2 h and 4 h: (a,d) untreated; (b,e) 2 h; and (c,f) 4 h.

4. Conclusions

To improve the charge-discharge performance of the ZrNi alloy, which had a high theoretical hydrogen storage capacity and low utilization because of the surface ZrO_2 passive layer, boiling alkaline

treatments for different periods of time were performed, and the electrochemical properties for the treated ZrNi alloys were examined.

The initial discharge capacities at 303 K for the ZrNi negative electrodes increased from 9 mAh·g⁻¹ to 24 mAh·g⁻¹ and 89 mAh·g⁻¹ after boiling alkaline treatments for 2 h and 4 h, respectively. Moreover, the initial discharge capacities at 333 K increased from 21 mAh·g⁻¹ to 114 mAh·g⁻¹ and 308 mAh·g⁻¹ after boiling alkaline treatments for 2 h and 4 h, respectively, and the high rate of dischargeability was also improved. The charge-transfer resistance was drastically decreased by the boiling alkaline treatment, and the dehydrogenation from ZrNiH₃ to ZrNiH was facilitated. SEM and EDX showed that the ZrO₂ passive layer on the ZrNi alloy surface was removed by the boiling alkaline treatment to form the porous morphology containing Ni(OH)₂, which would be converted to Ni during charging, leading to the improvement of the electrochemical properties of the ZrNi negative electrode. From these results, the modification of the ZrNi alloy surface with the boiling alkaline treatment is a useful approach to improve its electrochemical properties.

Acknowledgments: This work is financially supported by Aichi Steel Corporation.

Author Contributions: Akihiro Matsuyama designed the experiments and analyzed the results. Hironori Mizutani and Takumi Kozuka analyzed and interpreted the data. Hiroshi Inoue assisted in data analysis and manuscript preparation.

Conflicts of Interest: The authors declare no conflict of interest.

References

1. Boussami, S.; Khaldi, C.; Lamloumi, J.; Mathlouthi, H.; Takenouti, H. Electrochemical study of LaNi_{3.55}Mn_{0.4}Al_{0.3}Fe_{0.75} as negative electrode in alkaline secondary batteries. *Electrochim. Acta* **2012**, *69*, 203–208. [[CrossRef](#)]
2. Drulis, H.; Hackemer, A.; Flocik, L.; Giza, K.; Bala, H.; Gondek, Ł.; Figiel, H. Thermodynamic and electrochemical hydrogenation properties of LaNi_{5-x}In_x alloys. *Int. J. Hydrot. Energy* **2012**, *37*, 15850–15854. [[CrossRef](#)]
3. Sun, J.C.; Li, S.; Ji, S.J. The effects of the substitution of Ti and La for Zr in ZrMn_{0.7}V_{0.2}Co_{0.1}Ni_{1.2} hydrogen storage alloys on the phase structure and electrochemical properties. *J. Alloy. Compd.* **2007**, *446*, 630–634. [[CrossRef](#)]
4. Iwakura, C.; Kasuga, H.; Kim, I.; Inoue, H.; Matsuoka, M. Effect of alloy composition on electrochemical properties of the Zr-based Laves-phase hydrogen storage alloys. *Electrochim. Acta* **1996**, *41*, 2691–2694. [[CrossRef](#)]
5. Anik, M.; Karanfil, F.; Küçükdeveci, N. Development of the high performance magnesium based hydrogen storage alloy. *Int. J. Hydrot. Energy* **2012**, *37*, 299–308. [[CrossRef](#)]
6. Inoue, H.; Ueda, T.; Nohara, S.; Fujita, N.; Iwakura, C. Effect of ball-milling on electrochemical and physicochemical characteristics of crystalline Mg₂Ni alloy. *Electrochim. Acta* **1998**, *43*, 2215–2219. [[CrossRef](#)]
7. Kohno, T.; Yoshida, H.; Kawashima, F.; Inaba, T.; Sakai, I.; Yamamoto, M.; Kanda, M. Hydrogen storage properties of new ternary system alloys: La₂MgNi₉, La₅MgNi₂₃, La₃MgNi₁₄. *J. Alloy. Compd.* **2000**, *311*, L5–L7. [[CrossRef](#)]
8. Liao, B.; Lei, Y.Q.; Chen, L.X.; Lu, G.L.; Pan, H.G.; Wang, Q.D. A study on the structure and electrochemical properties of La₂Mg(Ni_{0.95}M_{0.05})₉ (M = Co, Mn, Fe, Al, Cu, Sn) hydrogen storage electrode alloys. *J. Alloy. Compd.* **2004**, *376*, 186–195. [[CrossRef](#)]
9. Guiose, B.; Cuevas, F.; Déamps, B.; Leroy, E.; Percheron-Guégan, A. Microstructural analysis of the ageing of pseudo-binary (Ti,Zr)Ni intermetallic compounds as negative electrodes of Ni-MH batteries. *Electrochim. Acta* **2009**, *54*, 2781–2789. [[CrossRef](#)]
10. Inoue, H.; Kotani, N.; Chiku, M.; Higuchi, E. High capacity hydrogen storage alloy negative electrodes for use in nickel-metal hydride batteries. *J. Alloy. Compd.* **2015**, *645*, S136–S139. [[CrossRef](#)]
11. Dantzer, P.; Millet, P.; Flanagan, T.B. Thermodynamic characterization of hydride phase growth in ZrNi-H₂. *Metall. Mater. Trans. A* **2001**, *32A*, 29–38. [[CrossRef](#)]
12. Cantrell, J.S.; Bowman, R.C., Jr.; Wade, L.A.; Luo, S.; Clewley, J.D.; Flanagan, T.B. Thermodynamic properties of and the degradation of ZrNiH_x at elevated temperatures. *J. Alloy. Compd.* **1995**, *231*, 518–523. [[CrossRef](#)]

13. Nei, J.; Young, K.; Regmi, R.; Lawes, G.; Salley, S.O.; Ng, K.Y.S. Gaseous phase hydrogen storage and electrochemical properties of Zr₈Ni₂₁, Zr₇Ni₁₀, Zr₉Ni₁₁ and ZrNi metal hydride alloys. *Int. J. Hydrol. Energy* **2012**, *37*, 16042–16055. [[CrossRef](#)]
14. Wakao, S.; Sawa, H.; Nakano, H.; Chubachi, S.; Abe, M. Capacities and durabilities of Ti-Zr-Ni alloy hydride electrodes and effects of electroless plating on their performances. *J. Less-Common Met.* **1987**, *131*, 311–319. [[CrossRef](#)]
15. Matsuoka, M.; Nakayama, E.; Uematsu, F.; Yamamoto, Y.; Iwakura, C. Activation mechanism of Ti_{0.5}Zr_{0.5}Ni_{1.3}V_{0.7}Mn_{0.1}Cr_{0.1} electrode in nickel-hydride batteries. *Electrochim. Acta* **2001**, *46*, 2693–2697. [[CrossRef](#)]
16. Züttel, A.; Meli, F.; Schlapbach, L. Surface and bulk properties of the Ti_yZr_{1-y}(V_xNi_{1-x})₂ alloy system as active electrode material in alkaline electrolyte. *J. Alloy. Compd.* **1995**, *231*, 645–649. [[CrossRef](#)]
17. Huang, H.; Huang, K.; Chen, D.; Liu, S.; Zhuang, S. The electrochemical properties of MgNi-x wt% TiNi_{0.5}Co_{0.44} ($x = 0, 10, 30, 50$) composite alloys. *J. Mater. Sci.* **2010**, *45*. [[CrossRef](#)]
18. Benavides, L.A.; Cuscueta, D.J.; Ghilarducci, A.A. MWCNT as mechanical support during ball milling of AB₅ alloy used as negative electrode of a Ni-MH battery. *Int. J. Hydrol. Energy* **2015**, *40*, 4925–4930. [[CrossRef](#)]
19. Mishima, R.; Miyamura, H.; Sakai, T.; Kuriyama, N.; Ishikawa, H.; Uehara, I. Hydrogen storage alloys rapidly solidification by the melt-spinning method and their characteristics as metal hydride electrodes. *J. Alloy. Compd.* **1993**, *192*, 176–178. [[CrossRef](#)]
20. Ikoma, M.; Komori, K.; Kaida, S.; Iwakura, C. Effect of alkali-treatment of hydrogen storage alloy on the degradation of Ni/MH batteries. *J. Alloy. Compd.* **1999**, *284*, 92–98. [[CrossRef](#)]
21. Yanagimoto, K.; Majima, K.; Sunada, S.; Sawada, T. Effects of surface modification on surface structure and electrochemical properties of Mm(Ni,Co,Mn,Al)_{5.0} alloy powder. *J. Alloy. Compd.* **2004**, *377*, 174–178. [[CrossRef](#)]
22. Li, H.W.; Inada, K.; Nakamori, Y.; Orimo, S.; Yakushiji, K.; Takanashi, K.; Ohyama, H.; Nakatsuji, K.; Dansui, Y. Size distribution of precipitated Ni clusters on the surface of an alkaline-treated LaNi₅-based alloy. *Acta Mater.* **2007**, *55*, 481–485. [[CrossRef](#)]
23. Gao, X.P.; Sun, Y.M.; Higuchi, E.; Toyoda, E.; Suda, S. Electrochemical properties and characteristics of the fluorinated Zr_{0.9}Ti_{0.1}V_{0.2}Mn_{0.6}Ni_{1.3}La_{0.05} electrode. *J. Alloy. Compd.* **1999**, *293*, 707–711. [[CrossRef](#)]
24. Parimala, R.; Ananth, M.V.; Ramaprabhu, S.; Raju, M. Effect of electroless coating of Cu, Ni and Pd on ZrMn_{0.2}V_{0.2}Fe_{0.8}Ni_{0.8} alloy used as anodes in Ni-MH batteries. *Int. J. Hydrol. Energy* **2004**, *29*, 509–513. [[CrossRef](#)]
25. Choi, W.K.; Yamataka, K.; Zhang, S.G.; Inoue, H.; Iwakura, C. Effects of surface treatment with boiling alkaline solution on electrochemical and physicochemical properties of the Zr_{0.9}Ti_{0.1}Ni_{1.1}Co_{0.1}Mn_{0.6}V_{0.2} alloy electrode. *J. Electrochem. Soc.* **1999**, *146*, 46–48. [[CrossRef](#)]
26. Matsuyama, A.; Mizutani, H.; Kozuka, T.; Inoue, H. Effect of surface treatment with boiling alkaline solution on electrochemical properties of the ZrNi alloy electrode. *Int. J. Hydrol. Energy* **2016**, *41*, 9908–9913. [[CrossRef](#)]
27. Cuevas, F.; Latroche, M.; Vigeron-Bourée, F.; Percheron, G.A. A conjoint XRD–ND analysis of the crystal structures of austenitic and martensitic Ti_{0.64}Zr_{0.36}Ni hydrides. *J. Solid State Chem.* **2006**, *179*, 3295–3307. [[CrossRef](#)]
28. Kuriyama, N.; Sakai, T.; Miyamura, H.; Uehara, I.; Ishikawa, H. Electrochemical impedance and deterioration behavior of metal hydride electrodes. *J. Alloy. Compd.* **1993**, *202*, 183–197. [[CrossRef](#)]
29. Poubaix, M. *Atlas Electrochemical Equilibria in Aqueous Solutions*, 2nd ed.; National Association of Corrosion Engineers (NACE): Houston, TX, USA, 1974; p. 333.
30. Senoh, H.; Ueda, M.; Inoue, H.; Furukawa, N.; Iwakura, C. Theoretical evaluation for thermodynamic stability of constituents of hydrogen storage alloy in concentrated alkaline solution at higher temperature. *J. Alloy. Compd.* **1998**, *266*, 111–117. [[CrossRef](#)]
31. Souza, L.M.M.; Kong, F.P.; McLarnon, F.R.; Muller, R.H. Spectroscopic ellipsometry study of nickel oxidation in alkaline solution. *Electrochim. Acta* **1997**, *42*, 1253–1267. [[CrossRef](#)]

